Research Square

Preprints are preliminary reports that have not undergone peer review.
They should not be considered conclusive, used to inform clinical practice,
or referenced by the media as validated information.

The RNA-binding protein SDOS regulates pro-survival autophagy in response to DNA damage in breast cancer cells

Anna Di Micco
University of Naples Federico II
Margherita Auriemma
University of Naples Federico II
Franca Esposito
University of Naples Federico II
Rosario Avolio
University of Naples Federico II
Danilo Swann Matassa
daniloswann.matassa@unina.it
University of Naples Federico II

Article

Keywords: SDOS, breast cancer, RNA-binding protein, DNA damage response, autophagy

Posted Date: September 9th, 2026

DOI: https://doi.org/10.21203/rs.3.rs-10832424/v1

License: This work is licensed under a Creative Commons Attribution 4.0 International License.
Read Full License

Additional Declarations: No competing interests reported.

Abstract

Purpose. Breast cancer is the most frequently diagnosed cancer and the second leading cause of death in women. In breast cancer cells, protein Syndesmos (SDOS, also known as TIRR, encoded by the NUDT16L1 gene) is a key regulator of 53BP1-mediated DNA damage response: its overexpression prevents 53BP1 function, leading to PARP inhibitor resistance in BRCA1-mutated tumors. SDOS is also an RNA-binding protein that associates with polysomes and regulates translation. Remarkably, SDOS-interacting RNAs reduce 53BP1 inhibition, indicating that both functions, i.e. SDOS function in 53BP1-mediated DNA damage response and RNA binding, are tightly coupled.

Methods. We used OOPS, RIP, polysome profiling, and PLA to characterize SDOS interactions with protein partners and RNA targets and to define the contribution of its cytoplasmic roles to the DNA damage response.

Results. We found that SDOS interacts with and regulates the activity of the major autophagy receptor SQSTM1/p62. At the same time, SDOS also regulates the translation of the SQSTM1 mRNA, ensuring stress-responsive translation upon DNA damage and sustained pro-survival autophagic response. Indeed, SDOS overexpression increases resistance to DNA-damage inducers, which is reverted by autophagy inhibition or SQSTM1 silencing. Notably, the Nudt16l1 and Sqstm1 genes are co-expressed in breast cancers but not in normal breast tissues, and the expression of both genes increases from normal to tumoral to metastatic tissues.

Conclusions. Herein, for the first time, evidence is provided for SDOS contribution to the DDR at multiple levels, through the regulation of transcripts encoding stress-responsive proteins and the riboregulation of their activity.

1. Introduction

Breast cancer (BC) is the most prevalent cancer globally, and the leading cause of cancer-related deaths among women[1]. BC staging and classification are determined by tumor size, nodal involvement, the presence of metastases, and specific biomarkers such as estrogen receptors, progesterone receptors, and the ERBB2 receptor (formerly HER2)[2]. Nonmetastatic breast cancer is treated with preoperative and postoperative systemic therapies that include chemotherapy, endocrine therapies, immunotherapy with monoclonal antibodies directed at tumor receptors, and surgery and radiation[3]. Besides being used to decrease tumor size before surgery, and administered after surgery to treat BC that express hormone receptors and ERBB2, chemotherapy is a core treatment for triple-negative BC (TNBC), because endocrine therapy and immunotherapy have no benefit[3].

One of the major risk factors for BC development is the presence of BRCA1/2 mutations, which cause genomic instability and cellular transformation. This led to the development of PARP inhibitors (PARPi), which induce cell death in BRCA-mutated cells through synthetic lethality, forcing the repair of the DNA damage through the error-prone Non-Homologous End Joining (NHEJ) repair pathway[4].

In the last decade, Syndesmos (SDOS, alias TIRR, encoded by the Nudt16l1 gene), a previously poorly characterized protein, has been at the epicentre of an intensive scientific discussion because of the identification of its regulatory role in DNA repair, through an interplay with 53BP1, the master regulator of double-strand DNA damage response (DDR) through NHEJ. Overexpression of SDOS prevents 53BP1 function by blocking its localization to double-strand breaks (DSBs), thus causing PARPi resistance in BRCA1-deficient cells[5]. However, SDOS is not only located in the nucleus, but also in the cytoplasm. Our group has demonstrated that SDOS is an RNA-binding protein (RBP) that interacts on the endoplasmic reticulum with the cancer-linked chaperone TRAP1[6], which is in itself a non-canonical RBP[7], and associates with actively translating ribosomes, and a consequent decrease in the rate of protein synthesis[8]. It is now evident that the two SDOS/TIRR functions are not separated, as RNA molecules are able to modulate SDOS/TIRR binding to 53BP1 and its recruitment to the DNA damage sites[9, 10].

This is particularly relevant, considering that most chemotherapeutic agents are DNA damage-inducing drugs, including those used for BC therapy, i.e. carboplatin and anthracyclines, as well as the recently introduced irinotecan/exatecan active metabolites SN-38 and DXd, which are the payloads of the antibody-drug conjugates (ADC) Sacituzumab govitecan and Trastuzumab deruxtecan respectively[11].

Several mechanisms have been described to account for different degrees of sensitivity to chemotherapy in patients, and for the development of drug resistance. Among those, increased DDR capabilities, resistance to apoptosis and enhanced pro-survival stress response mechanisms. In this view, one notable mechanism enacted by cancer cells to quickly adapt and evade most therapies is autophagy, a catabolic process designed to recycle damaged cellular components and provide energy [12]. Evidence has been accumulating to suggest that autophagy and DDR are actually mechanistically linked despite occurring in spatially distinct cellular compartments. A very recent, high-profile work demonstrated that lysosomes directly process topoisomerase 1 cleavage complexes DNA lesions through a selective autophagy process, protecting genome stability in response to clinically relevant doses of topoisomerase 1 inhibitors[13].

Of note, our previous data suggested that the autophagy receptor SQSTM1/p62 is one of the SDOS protein partners, and that SDOS could also bind the SQSTM1 mRNA [8]. Notably, it has been recently demonstrated that SQSTM1 itself is a noncanonical RBP, whose activity is modulated by its binding to vault RNAs (vtRNAs)[14]. Interestingly, these vault RNAs are putative SDOS targets[8].

Starting from these observations, we investigated for the first time the function of SDOS in the autophagic response to DNA damage, and found that SDOS contributes to the activation of this process. Indeed, SDOS binds SQSTM1/p62, modulating its activation, but at the same time ensures stress-responsive translation of the SQSTM1 mRNA, to provide a prolonged autophagic response upon DNA damage. This increases resistance to DNA damage inducers, which can be counteracted by autophagy inhibition.

2. Methods

2.1 Cell culture and transfections

Human MCF7 and HCC1937 breast carcinoma cells were cultured in DMEM and RPMI 1640 medium, respectively, at 37°C, 5% CO_2. Culture media were supplemented with 10% fetal bovine serum, 1.5 mmol/L glutamine and Normocin (Invivogen Cat. code ant-nr-05). Both cell lines were acquired from the CEINGE- CEINGE Biotecnologie Avanzate - Franco Salvatore cell culture facility, where they are periodically authenticated using the ATCC cell STR profile system.

For transient silencing of SDOS, we used siRNAs purchased from Qiagen: SDOS-directed siRNAs (cat. no. SI00713293) and nontargeting control siRNA (cat. no. SI03650318), whereas for transient silencing of SQSTM1, we used ON-TARGETplus siRNA (Dharmacon). Transfections were performed using Lipofectamine™ RNAi MAX (Invitrogen™), according to the manufacturer's protocol.

2.2 Generation of MCF7 inducible clones

The MCF7 Flp-In T-Rex cells were kindly gifted by Prof. Reuven Agami (Netherlands Cancer Institute). These cells were obtained by transfection with a PFRT/lacZeo plasmid, containing an FRT recombination site along with the gene for Zeocin resistance under the control of a strong promoter, and subjected to a first clonal selection. A second transfection was performed to obtain clones co-integrated with the pcDNA6/TR plasmid containing the gene for Blasticidin resistance and allowing the expression of the tetracycline repressor under the control of the CMV promoter. These clones are therefore equipped with a recombination site for the insertion of genes of interest controlled by an inducible promoter. Starting from these cells, we generated tet-inducible clones expressing shRNAs against SDOS (shSDOS) and a corresponding nonsilencing control (shNS), to obtain SDOS knock-down (KD), and cells expressing a flag-HA-tagged SDOS protein (SDOS-flag) and, as a control, cells expressing a flag-HA-tagged H3 histone (H3C2-flag). To this aim, we generated a construct containing an shSDOS sequence or an shNS under the control of the U6 promoter, which is a type III RNA polymerase III promoter commonly used for driving shRNA expression in vector-based RNAi. Short hairpin sequences used (between the BglII-KpnI restriction sites in pFRTU6tetO) are:

NS=agatctGTCTCGCTTGGGCGAGAGTAAGCCTGACCCACTTACTCTCGCCCAAGCGAGACTTTTTggtacc;
SDOS=agatctGCCTCAGGATGCTCTTGTTTATCCTGACCCAATAAACAAGAGCATCCTGAGGCTTTTTggtacc.
H3-Flag and SDOS-Flag are expressed under the control of the CMV promoter. All the plasmids contained a tetracycline-regulated operator. The plasmids thus obtained and the pOG44 plasmid expressing Flp recombinase were further transfected into the Flp-In-T-Rex MCF7 clones. The sequence for the hygromycin resistance gene contained near the FRT recombination site allows clone selection, while the Flp recombinase encoded by the pOG44 plasmid, which is co-transfected with the construct of interest, is essential for homologous recombination between the FRT sites and the insertion of the gene of interest. The cells were then selected with 150 ug/mL of Hygromycin, which we found to be the minimal lethal concentration.

2.3 Western blot and immunoprecipitation

Equal amounts of protein from cell lysates were subjected to SDS-PAGE and transferred to a PVDF membrane (Merck, IEVH85R). Membranes were blocked in a 5% milk in TBS-Tween solution for 1 h at room temperature. The following antibodies were used: from Santa Cruz Biotechnology anti-ACTIN (sc-47778), anti-GAPDH (sc-69778), anti-RPS6 (sc-74459), anti-RPL19 (sc-100830), anti-VINCULIN sc-73614, anti-SQSTM1 (sc-28359), anti-HSP27 (sc-13132), from Millipore anti-puromycin (MABE343), from Novus Biologicals anti-LC3B (NB3868), from Proteintech anti-hnRNPC (11760-1-AP), from Atlas antibodies SDOS (HPA044186), from Genetex LSM14A (GTX120187), from ABclonal anti-MT-ATP6 (A17960). All primary antibodies were incubated overnight at 4°C. Anti-mouse (Bethyl Laboratories, A90-137P) and anti-rabbit (Bethyl Laboratories, A120-108P) antibodies were used at a 1:20,000 dilution and incubated for 1 h at room temperature. Images were acquired with a ChemiDoc MP Imaging System (Bio-Rad), and where indicated, protein levels were quantified by densitometric analysis using the software ImageJ[15].

Immunoprecipitations were performed by incubating equal amounts of total lysates, obtained as described above, with the indicated antibodies overnight. Subsequently, 30 µL of Dynabeads Protein G (Thermo Fisher Scientific cat. no 10003D) were added to each sample and incubated for two hours at 4°C. Beads were magnetized and washed three times with lysis buffer and for a final wash with PBS, then directly denatured in Laemmli sample buffer and loaded for Western Blot.

2.4 Polysome profiling and analysis of polysome-associated mRNA

Following 48h of induction of the shRNA expression with Tetracyclin in MCF7 FITR, or transfection with SDOS directed siRNA or control siRNA in HCC1937, cells were washed with ice-cold PBS supplemented with 100 µg/mL cycloheximide and resuspended in 500 µL of lysis buffer (10 mM Tris-HCl at pH 7.4, 100 mM KCl, 10 mM $MgCl_2$, 1% Triton X-100, 1 mM DTT, 10 U/mL RNaseOUT [Invitrogen, 10777019], 100 µg/mL of cycloheximide) with and protease inhibitors (cOmplete, EDTA-free Protease Inhibitor Cocktail Tablets, Roche, product code 11 873 580 001). After 10 min of incubation on ice, cell lysate was centrifuged for 10 min at 14,000 rpm at 4°C. The supernatant was collected, and protein concentration was determined using a Bradford assay (Bio-Rad). Equal amounts of protein were loaded onto a 10%–60% sucrose gradient obtained by adding 6 mL of 10% sucrose over a layer of 6 mL of 60% sucrose prepared in lysis buffer, in a 12 mL Open-Top Thinwall Ultra-Clear Tube (Beckman, 344059). Gradients were prepared using a gradient maker (BioComp). Polysomes were separated by centrifugation at 37,000 rpm for 2 h using a Beckman SW41 rotor. Twelve fractions of 920 µL were collected, and polysomes were monitored by following the absorbance at 254 nm.

Proteins were isolated by adding TCA (15% final concentration) to each fraction and left overnight at -20°C. Fractions were then centrifuged a 10k xG for 15 min at 4°C and washed twice with cold acetone. Protein pellets were directly resuspended in Laemmli and loaded for Western Blot.

As for the analysis of polysome-associated mRNA, following the addition of 50 pg of Luciferase RNA as an internal control to each fraction, RNA extraction was performed by adding TRIzol to the fractions at a 1:1 v/v ratio following the manufacturer's instructions. The same volume of RNA from each fraction was

reverse transcribed to cDNA and used for qPCR assays (see “RNA extraction and RT-qPCR”). RNA amounts were quantified, normalized to internal Luc as control, summed across all fractions, analyzed, and presented after normalized to their total RNA concentrations.

2.5 Ribosome Isolation

Ribosome isolation was performed as described in[16]. Briefly, cells were lysed using NP40-buffer (0,3% NP-40, 10 mM $MgCl_2$, 100 mM KCl, 30 mM Tris- HCl pH 7.4, 100 µg/mL cycloheximide, 1mM DTT, 30U/ml RNaseOUT™, cOmplete, EDTA-free Protease Inhibitor Cocktail Tablets, Roche, product code 11 873 580 001). The lysates were incubated for 5 minutes at 4°C and then centrifuged for 15 minutes at 10,000 g at 4°C. The supernatants were loaded over a 20% sucrose cushion with cycloheximide and centrifuged for 2 hours at 149,000 g at 4°C. The pellets were processed for a Western blot analysis.

2.6 Orthogonal Organic Phase Separation (OOPS)

OOPS was performed as described in[17]. Briefly, cells were UV cross-linked on ice at 150 mJ/cm^2 with UV light at 254 nM. Then, cells were washed twice with PBS and immediately lysed by scraping in TRIzol (Thermo Fisher Scientific, 15596018). The homogenate was transferred to a new tube and incubated at RT for 5 min to dissociate unstable RNA–protein interactions. For biphasic extraction, 200 µL of chloroform (Sigma-Aldrich, 319988) was added, and samples were centrifuged for 15 min at 12,000g at 4°C. The upper, aqueous phase (containing non-cross-linked RNAs) and the lower, organic phase (containing non-cross-linked proteins) were discarded, and the interface (containing the protein–RNA adducts) was subjected to two more AGPC phase separation cycles, precipitated by the addition of nine volumes of methanol, and pelleted by centrifugation at 14,000g, RT for 10 min. For RNA-binding protein analyses, the precipitated interface was resuspended in 100 µL of 100 mM triethylammonium bicarbonate (TEAB) and 1% SDS, sonicated using a bioruptor (Diagenode) for 15 cycles of 30 sec (ON/OFF), high setting, at 4°C, incubated at 95°C for 20 min, cooled and digested with 2 µL RNase A/T1 (Thermo Fisher Scientific, EN0551) overnight at 37°C. The following day, after a final cycle of AGPC phase partitioning, proteins were released and recovered from the organic phase by methanol precipitation and analyzed by western blot.

2.7 Proximity Ligation Assay (PLA)

In situ PLA was performed using the NaveniFlex Cell kit (Art.no 60017 Atto647N, Navinci Diagnostics AB, Sweden) according to the manufacturer’s instructions. Briefly, cells were seeded on coverslips, fixed, permeabilized, and hybridized with primary antibodies. For negative controls, only one of the two primary antibodies has been used. Cells were subsequently hybridized with secondary antibodies conjugated with the PLA probes (PLUS and MINUS) and then subjected to ligation and rolling circle amplification using fluorescently labeled oligonucleotides. Cells were washed, incubated for 5 min in PBS containing 0.2 µg/mL of DAPI (D1306, Thermo Fisher Scientific), to allow nuclei detection, washed and mounted on slides using PBS glycerol 1:1 as mounting medium. The following antibodies were used: anti-SQSTM1 (FineTest FNab06087), anti-FLAG (Merck F1804), anti-puromycin (EMD Millipore MABE343), ant-phosphoRPS6 (Cell Signaling #2215). Image acquisition was performed by using the Leica Thunder

imaging system (Leica Microsystems) equipped with a Leica DFC9000GTC camera and a PlanApo 63× oil-immersion (NA 1.4) objective lens. A fluorescence LED light source and appropriate excitation and emission filters were used. Images were acquired by taking Z-slices from the top to the bottom of the cell by using the same settings (LED source power, exposure time) and the small volume computational clearing (SVCC) mode for the different cell lines and in all experimental conditions.

Fluorescence intensity measurements were performed using ImageJ[15].

2.8 Subcellular fractionation

To perform nuclear-cytoplasmic fractionation, approximately 1M cells were harvested and resuspended in 250 µL of hypotonic buffer (10 mM HEPES pH 7.9, 1.5 mM $MgCl_2$, 10 mM KCl, protease inhibitors). Samples were passed 12 times through a syringe needle (27G), left on ice for 30 minutes and then centrifuged at 1000 xG for 10 minutes at 4°C. Supernatants containing cytosolic proteins were centrifuged at 20k xG for 10 minutes at 4°C to eliminate debris. The nuclear pellets were washed twice with hypotonic buffer and resuspended in 50 µL of lysis buffer (5 mM HEPES, 1.5 mM $MgCl_2$, 300 mM NaCl, 0.1 mM EDTA, 26% Glycerol, Protease inhibitors), incubated on ice for 20 minutes and further centrifuged at 20k xG for 10 minutes at 4°C. Pellets were discarded, supernatants contained soluble nuclear proteins.

2.9 RNA extraction and RT-qPCR

Total RNA extraction procedures were performed using TRIzol, following the manufacturer's instructions. For first-strand synthesis of cDNA, 1 µg of RNA was used in a 20 µL reaction mixture using the All-In-One 5X RT MasterMix with gDNA Removal (Abm, G592). For real-time PCR analysis, 20 ng of cDNA sample was amplified by using the BlasTaq 2X qPCR Master Mix (Abm, G891) in a CFX96 Touch Real-Time PCR Detection System (Bio-Rad). The reaction was performed at 95◦C for 2 min, followed by 40 cycles of 5 s at 95◦C and 30 s at 60◦C. The primers used are listed below:

PPIA fw: CTGCACTGCCAAGACTGA

PPIA rv: GCCATTCCTGGACCCAAA

Luc fw: TACAACACCCCAACATCTTCGA

Luc rv: GGAAGTTCACCGGCGTCAT

SQSTM1 fw: AGGAAACTGGAGCCCACGTC

SQSTM1 rv: GGCTTCTTTTCCCTCCGTGC

SDOS fw v1specific: CACGGCCTGGAGGTGCT

SDOS rv v1specific: CAGCTTCTCCTCGGGCATC

MT-ATP8 fw: ACTACCACCTACCTCCCTCAC

MT-ATP8 rv: GGATTGTGGGGGCAATGAATG

MT-CO1: AATCATCGCTATCCCCACCG

MT-CO1: CAGAGCACTGCAGCAGATCA

vault RNA 1–1 fw: TTAGCTCAGCGGTTACTTCGACAGTTC

vault RNA 1–1 rv: AAAAGGACTGGAGAGCGCCC

vault RNA 1–2 fw: GGCTGGCTTTAGCTCAGCGG

vault RNA 1–2 rv: AAAAGAGCTGGAAAGCACCC

vault RNA 1–3 fw: AGCGGTTACTTCGCGTGTCATC

vault RNA 1–3 rv: AAGAGGGCTGGAGAGCGCC

NEAT1_1 fw: GGAGAGGGTTGGTTAGAGAT

NEAT1_1 rv: CCTTCAACCTGCATTTCC

2.10 RNA immunoprecipitation (RIP)

MCF7 cells (shNS/shSDOS) were treated with etoposide for 4 hours, and then chemical crosslinking was performed using formaldehyde (0.1%) to crosslink proteins and RNA. Cells were lysed using RIP buffer (40 mM Tris-HCl pH 7.5, 2 mM EDTA, 300 mM NaCl, 1% NP-40, 1mM DTT, RNase inhibitors: RNaseOUT™ Recombinant Ribonuclease Inhibitor, Invitrogen™, product code 10777019) and protease inhibitors (SIGMAFAST™ Protease Inhibitor Tablets, product code S8820). Subsequently, the cells were incubated with anti-SQSTM1 antibody for 18 hours and then the antigen-antibody complexes were isolated by adding Dynabeads Protein G (Invitrogen) to the solution for 2 hours. The Dynabeads Protein G were resuspended in proteinase K buffer containing 100mM pH 7.4 Tris-HCl, 50mM NaCl, 10mM EDTA, 1% SDS and RNaseOUT™. At this point, luciferase mRNA as a spike-in control was added along with Proteinase K (Thermo Scientific™, product code 11501515). The sample was incubated at 55°C for 30 minutes at 1400 rpm. The RNAs were extracted using TRIzol protocol.

2.11 Bioorthogonal Non-Canonical Amino Acid Tagging (BONCAT) and pulldown of newly sinthesized proteins

L-Homopropargylglycine (HPG, Thermo Fisher Scientific Cat. n C10186) labeling was performed as follows: following silencing by transfection of SDOS-directed siRNAs for 48 hours, cells were incubated in cysteine/methionine-free medium (Sigma-Aldrich) for 30 min at 37°C, and then 100 μM HPG was added to the media for 1 hour at 37°C. Cells were detached, centrifuged and resuspended in 50 μL of

Click-iT lysis buffer (50mM Tris-HCl pH 8, 1% SDS, 250 U/mL Universal Nuclease (Thermo Fisher Scientific Cat. n. 88702)) and incubated on ice for 15 min. Extracts were sonicated using a Bioruptor (Diagenode) for 5 cycles of 30 sec (ON/OFF), high setting, at 4°C, and centrifuged at 18,000 xG for 5 min, and protein concentrations were determined by BCA assay (Thermo Fisher Scientific). 400 µg of proteins from each sample were subjected to a click reaction using a commercial kit (Click-iT protein reaction buffer kit; Thermo Fisher Scientific Cat. n. C10276), with 40 µM Biotin-azide (PEG4 carboxamide-6-Azidohexanyl Biotin, Thermo Fisher Scientific Cat. n. B10184), according to the manufacturer's protocol. After the end of the click reaction, proteins were purified from the mixture using a Methanol/chloroform approach. The extracted pellet was dissolved in 200 µL of 50 mM Tris-HCl pH 8, 4% SDS, 10 mM EDTA and protease inhibitors, and protein concentrations were determined by BCA assay. Samples were then diluted 1:4 to reduce SDS concentration and prevent any interference with biotin-streptavidin binding, to obtain a solution containing 20 mM Tris-HCl pH 8, 100mM NaCl, 10 mM $MgCl_2$, 0,1% Triton, 0,05 mg/mL BSA (as in[18]). Equal amounts of biotinylated (newly synthesized) proteins were isolated by incubation with 50 µL of Dynabeads MyOne Streptavidin C1 (Thermo Fisher Scientific Cat. n. 65002) overnight at 4°C with rotation. Beads were magnetized and washed 3 times with high-salt buffer (TBS + 500 mM NaCl + 0.1% IGEPAL CA-630) followed by a final wash in TBS + 0.05% Tween-20, then denatured in Laemmli sample buffer and loaded for Western Blot using anti-biotin antibodies (Invitrogen anti-Biotin Cat. n. 31852).

2.12 Viability assays

shNS, shSDOS, H3-flag and SDOS-flag MCF7 cells were seeded in 96-well plates (2500 cells/well) in a final volume of 100 µL, and induced with Tetracycline. 48 hours post-seeding, cells were treated with Etoposide 40 µM for a further 48 hours. The 10 µL alamarBlue HS Cell Viability Reagent (Invitrogen, A50101) was added to the culture medium. After 2 h incubation at 37°C, fluorescence intensity of resorufin was measured using a Synergy H1 microplate reader (BioTek).

2.13 Bioinformatic analyses and statistics

GraphPad Prism 9 (version 9.3.1) software was used for statistical data analysis. Bar graphs display mean ± SEM and all data points. Experimental replicates and the applied statistical tests are mentioned in the figure legends. Expression analyses in tumors were performed using GEPIA2[19].

3. Results

3.1 SDOS binds RNA and active ribosomes in breast cancer cells

In order to unveil other SDOS roles and to correlate its cytosolic function (as an RBP and translational regulator) with its nuclear function (as a regulator of DNA repair systems), we performed polysome profiling to look for potential changes in the regulatory activity of SDOS on protein synthesis in response to DNA damage: inducible SDOS knock-down (KD) MCF7 cell clones (shSDOS) and respective controls

(shNS) were treated with 40 μM etoposide for 4-hours (Fig. 1A). Quantification of the profiles obtained showed no difference in the total amount of polysomes with respect to SDOS expression levels (Fig. 1B). However, in both SDOS-silenced and SDOS-expressing cells, polysomes were significantly reduced in response to genotoxic stress, compared with their respective untreated controls (Fig. 1B). To assess the quality of the preparation and validate the binding of SDOS to actively translating polysomes the resulting fractions were then processed for Western blot analysis. Results show that SDOS is present in all ribosomal fractions, but its binding is reduced following treatment, either as a result of dissociation or of reduction of their abundance (Fig. 1C). These data confirm that SDOS presence in polysomal fractions is closely related to ribosomal activity. The quality of our preparation is testified by the enrichment of the two ribosomal small (RPS6) and large (RPL19) subunits, mirrored by the absence, in the polysomal fractions (7–11), of an unrelated cytosolic protein (GAPDH) (Fig. 1C). Similar results were obtained in HCC1937 breast cancer cells following siRNA-mediated SDOS silencing (Supplementary Fig. S1A). SDOS association to ribosomes was further confirmed by isolating bulk ribosomes from MCF7 cells (Supplementary Fig. S1B), whereas proximity ligation assays (PLA) allowed us to demonstrate that SDOS binds actively translating polysomes, marked by phosphorylated (active) ribosomal protein S6 (Fig. 1D), with cycloheximide (CHX) treatment, which freezes polysomes in their position on the mRNAs, intensifying the PLA signal. These data are in accordance with a dual subcellular localization of the SDOS proteins in BC cells, as previously shown in HeLa cells [8]. To confirm this, we performed subcellular fractionations in both MCF7 cells and HCC1937, an epithelial ductal BC cell line carrying BRCA1 mutation, which showed a significant cytosolic localization of the protein, along with its expected nuclear localization (Fig. 1E). In this regard, it is worth noting that, according to the Human Protein Atlas [20] database, SDOS/NUDT16L1 shows a “general cytoplasmic expression with a granular pattern”.

To also confirm that SDOS retains its RNA-binding capabilities in the analyzed cellular systems, we applied the Orthogonal Organic Phase Separation (OOPS) technique in MCF7. The analysis revealed the presence of SDOS in the RBP compartment and, therefore, its binding to the RNAs (Fig. 1F). Interestingly, etoposide treatment reduced SDOS binding to mRNAs.

(A) Polysome profiling, with absorbance measurement at 254 nm, of MCF7 clones silenced for SDOS (shSDOS) and its control shNS, in the presence and absence of 4-hour treatment with 40 μM etoposide (Eto). The peaks in the profile, from left to right, reflect ribosomal protein complexes with increasing density: free ribonucleoproteins, small (40S) and large (60S) ribosomal subunits, monosomes (80S), and polysomes. The area under the curve corresponding to fractions 5 and 6 represents the monosomes, while the area from fractions 7 to 12 indicates the polysomes. (B) The graph shows the polysome/monosome ratio as a measure of translational activity. The numbers on the bars indicate statistical significance, calculated using Student's t-test (n = 3). (C) Western blot analysis of fractions extracted from the polysome profiling of untreated MCF7 shNS cells (NT) and cells treated for 4 hours with etoposide 40 μM (Eto), along with their respective inputs (IN). Probing was performed with anti-GAPDH, representing a cytosolic protein that should not be associated with polysomes, anti-RPS6, as a marker of the ribosomal small subunit, anti-RPL19 as a marker of the ribosomal large subunit, and anti-SDOS antibodies. (D) Representative image of PLA showing the interaction of SDOS-flag with

phosphorylated (active) ribosomal protein S6 (phosphoRPS6) in MCF7 cells following 24 h induction of SDOS-flag by using anti-FLAG and anti-phosphoRPS6 antibodies. Positive signals of interaction are shown as pink dots, nuclei are stained with DAPI (blue). Cycloheximide (CHX) treatment (100 µg/mL, 30 min) was used to stabilize the binding ribosome and increase binding. Scale bar: 20µm. E) Subcellular fractionation performed in MCF7 (left) and HCC1937 (right) BC cells, to identify total (tot), cytosolic (C) and nuclear (N) pools of the SDOS protein. Lamin A/C have been used as nuclear markers, HSP27 has been used as a cytosolic marker. F) Representative western blot of OOPS samples after 4-hour treatment with etoposide (40 µM) and respective inputs. Vinculin and Actin were used as negative controls (being proteins that do not bind RNAs), while the two canonical RBPs LSM14A and hnRNPC were used as positive controls, to confirm quality of RBP isolation.

3.2 SDOS binds the SQSTM1/p62 protein

Our previous quantitative proteomics analyses identified SQSTM1/p62 as a putative SDOS protein partner. Considering that this protein is involved in the regulation of autophagy[20], one of the main survival mechanisms employed by cells under stress conditions, including genotoxic stress [12], we sought to investigate the protein-protein interaction between SDOS and SQSTM1 in BC cells in response to DNA damage. Co-immunoprecipitation (co-IP) assays confirmed that SDOS interacts with SQSTM1 in both MCF7 (Fig. 2A) and HCC1937 (Fig. 2B) cells, validating the protein-protein interaction suggested by mass spectrometry in HeLa cells[8]. Interestingly, coIPs showed that the binding between the two proteins is decreased by DNA damage induced by either carboplatin or etoposide (Fig. 2A-B). PLA performed in MCF7 cells further confirmed the binding between the two proteins, and the reduced interaction following carboplatin treatment as well (Fig. 2C). To confirm that the two proteins undergo different fates following DNA damage-induced autophagy, we treated cells with etoposide to induce DNA damage. As expected, we observed a marked reduction in SQSTM1 expression following etoposide, due to the fact that SQSTM1 is degraded by the same autophagosomes of which it has promoted formation, testifying its activation, whereas SDOS expression remains unchanged (Fig. 2D). This confirms that SDOS is not degraded via autophagy, and that the interaction between the two proteins is disrupted upon SQSTM1 activation. Interestingly, this experiment also shows a significantly higher expression of SQSTM1/p62 in SDOS KD cells compared to controls in basal conditions, but that, following prolonged treatment times, its levels are dramatically reduced, especially upon SDOS silencing (Fig. 2D, right panel). This suggests that SDOS expression impacts both SQSTM1/p62 expression and activation. We therefore decided to investigate both aspects.

A) MCF7 cells were treated for 4 hours with Carboplatin (400 µM), harvested and total lysates were immunoprecipitated with anti-SQSTM1 antibodies. VINCULIN was used as a loading control. B) HCC1937 cells were treated with etoposide (20 µM) for 1 hour, harvested, and total lysates were immunoprecipitated with anti-SQSTM1 antibodies. ACTIN was used as a loading control. C) Representative image of PLA showing the interaction of SDOS-flag with SQSTM1/p62 in MCF7 cells following 24 h induction of SDOS-flag using anti-FLAG and anti-SQSTM1 antibodies. Positive signals of interaction are shown as pink dots, nuclei are stained with DAPI (blue). Scale bar: 20µm. D)

Representative Western blot of shNS and shSDOS samples treated with etoposide (40 μM) for 16 hours, compared to their respective untreated controls. Vinculin was used as a normalizer. LC3B was used as an autophagy marker. The bar graph shows mean ± SEM of densitometric quantification of normalized SQSTM1 bands in three replicates. Asterisks represent the statistical significance based on a Student's t-test. *= $p < 0.05$; ***= $p < 0.001$.

3.3 SDOS regulates SQSTM1 through its binding to vault RNAs and regulates its activation

Recent studies have demonstrated that SQSTM1 activity is regulated at multiple levels, from post-translational modification to riboregulation. Specifically, it has been shown that SQSTM1 itself is a non-canonical RBP and that the small noncoding vault RNAs inhibit its function[14]. Interestingly, vault RNAs have also been found to bind SDOS[8]. We therefore hypothesized that SDOS-SQSTM1 protein-protein interaction could affect their reciprocal binding to vtRNAs and, in turn, SQSTM1 autophagic activity. We therefore performed an RNA immunoprecipitation (RIP) experiment, which revealed that SQSTM1/p62 and vtRNA1-1 binding is significantly decreased upon etoposide treatment (Fig. 3A). This finding indicates SQSTM1/p62 activation, in both shNS and shSDOS cells. Intriguingly, our data show that vtRNA 1–2 is also bound to SQSTM1 in these cells; however, its regulation is different from that of vtRNA 1–1 and deserves further research. As a control, we used the unrelated PPIA mRNA showing no significant enrichment in our RIPs, thus confirming the specificity of vtRNA 1–1 and vtRNA 1–2 binding to SQSTM1. Conversely, vtRNA 1–3 does not seem to bind SQSTM1. To investigate the hypothesis that SDOS binding to vtRNAs could be involved in SQSTM1 activity regulation, we also performed RIP assays In MCF7 cells expressing the SDOS-flag protein under the control of tetracycline. This showed that SDOS binds vtRNA 1–1 only upon DNA damage, suggesting that SDOS could contribute to SQSTM1 activation by sequestering vtRNA 1–1 upon DNA damage (Fig. 3B). Again, the negative control, the MT-CO1 mRNA, which is a mitochondrial genome-encoded transcript, and therefore restricted to the organelle, was not enriched at all, while the positive control NEAT1, which is a well-characterized interactor[10], is dramatically enriched, confirming the efficacy of the assay. Moreover, the RIP results are not affected by vtRNA expression levels: indeed, RT-qPCRs confirm that their expression, as well as SQSTM1 mRNA expression, is not significantly affected by either SDOS silencing or etoposide (Fig. 3C), as all the transcripts are below a nonstringent fold change cutoff of 1.5, although a few show statistically significant small differences. In conclusion, these data suggest that SDOS could favor vtRNA 1–1 detachment from SQSTM1 upon DNA damage, an event that allows SQSTM1 activation.

Notably, the SQSTM1 transcript was itself among the SDOS mRNA targets previously identified by iCLIP-seq in HeLa cells[8]. However, as shown in Fig. 3B, our RIP assays showed no enrichment of the SQSTM1 transcript in the SDOS IP.

A) RIP-qPCR assays performed in shNS and shSDOS cells treated for 1 hour with 40 μM etoposide. The data are represented as mean ± SEM of three independent experiments. B) RIP-qPCR assays performed in SDOS-flag MCF7 cells treated for 4 hours with 400 μM Carboplatin. The data are represented as mean

± SEM of five independent experiments. C) RT-qPCR of total RNAs extracted from shNS/shSDOS MCF7 cells, after 72 hours of induction followed (where indicated) by a 4-hour etoposide treatment (40 μM). Data represent mean ± SEM of four independent experiments. Asterisks show statistical significance (*p < 0.05; **p < 0.01) based on the Student's t test.

3.4 SDOS regulates stress-responsive translation of the SQSTM1 mRNA

A direct binding between the SQSTM1 transcript and the SDOS protein could not be confirmed; however, especially for non-canonical RBPs like SDOS[21], the binding to target RNA can be very dynamic. For this reason, considering the role exerted by SDOS in translation control, and the altered SQSTM1/p62 protein expression upon SDOS KD (Fig. 2D), in the absence of any change in mRNA levels Fig. 3C), we decided to explore the hypothesis that SDOS could exert a translational control over the SQSTM1 mRNA. To this aim, we first performed a polysome profiling analysis on shNS and shSDOS MCF7 cells under basal conditions and after a 4-hour treatment with etoposide (40 μM) and extracted RNAs from each fraction, in order to quantify by RT-qPCR the distribution of mRNA in the cell, and therefore its translation efficiency. As a control gene, we used PPIA, a housekeeping gene that is not bound by SDOS according to our iCLIP data. As shown in Fig. 4A, we detected higher SQSTM1 mRNA association with polysomes in SDOS KD cells, indicating increased translation following SDOS silencing. However, SQSTM1 mRNA translation is reduced by etoposide in shSDOS cells, while sustained in shNS controls, suggesting that SDOS may act as a translational repressor under resting conditions, to then allow the release of protected mRNAs for stress-responsive translation. Indeed, the unrelated PPIA mRNA does not show any differences between shNS and shSDOS cells, but only a slight decrease in translation efficiency following etoposide, in line with the global translational response to etoposide (Fig. 1A). To confirm our hypothesis, we performed puro-PLA experiments, which indeed showed that in standard conditions, shRNA-mediated SDOS silencing determines an increase in the number of puromycilated (nascent) chains of SQSTM1, indicating augmented translation (Fig. 4B). However, following etoposide treatment, SDOS-expressing cells respond by increasing the translation of SQSTM1, which SDOS knock-down cells are incapable of (Fig. 4B). Finally, the increased SQSTM1 protein synthesis upon SDOS silencing was further corroborated by a BONCAT assay (Fig. 4C). In summary, these results suggest that SDOS acts a translational repressor of SQSTM1 activity under basal conditions while modulating the response to DNA damage by allowing more efficient translation of SQSTM1 under genotoxic stress conditions.

A) Distribution of the mRNAs in a polysome profile. Data are represented as mean ± SEM of three independent experiments and have been obtained by amplifying by RT-qPCR the indicated transcripts from every single fraction collected in a polysome profiling experiment and calculating the percent distribution of the transcript along the gradient. 100 pg of Luciferase mRNA have been added as a spike-in control to each fraction and later used as a reference in the RT-qPCR assay. Fractions 7–11 represent the active polysomal fractions. B) Representative image (left) and fluorescence intensity quantification (right) of puro-PLA performed by adding low doses of puromycin (1 μg/mL) for 10 minutes to shNS and shSDOS MCF7 cells following treatment with etoposide (40 μM, 4h) and controls before fixation. Pink

dots represent the puromycylated nascent chains of the SQSTM1 protein. Nuclei are stained with DAPI (blue). Scale bar: 10μm. The bar graph shows fluorescence intensity quantification represented as mean ± SEM of 6 fields from two biologically independent replicates. Numbers above bars show statistical significance (p-values) on an unpaired t-test.

3.5 SDOS regulates SQSTM1/p62 activity in genotoxic stress conditions

To verify the effects of the regulation of both SQSTM1 expression and activity, and with the aim of investigating the role of SDOS in autophagy, we assessed the expression of SQSTM1 and the lipidation level of LC3B following etoposide treatment (40 μM) in SDOS KD cells and controls. Western blot analysis again showed that the steady-state level of SQSTM1 is increased upon SDOS KD, in accordance with its increased translation (Fig. 5A). Indeed, treatment with CHX, which inhibits translation, completely abolishes such differences. Following etoposide treatment, SQSTM1 expression is reduced as proof of its activation, as confirmed by increased lipidation of the well-known autophagy marker LC3B. As mentioned above, the reduction in SQSTM1 expression is a common indicator of autophagy activation[20], since SQSTM1 itself is directed to the autolysosomes once the autophagic process has been activated by its binding to ubiquitinated proteins [22]. Consistent with our model, long-term treatment with etoposide leads to a more pronounced reduction of SQSTM1 expression in SDOS KD cells, in which stress-responsive re-synthesis of SQSTM1 is compromised (Fig. 5A). Again, this is confirmed by co-treatment with CHX, which led to a marked reduction of SQSTM1 levels and abolished the differences between shNS and shSDOS cells, thus confirming that SDOS facilitates translation of SQSTM1 in response to DNA damage, ensuring sustained expression and autophagic response.

To confirm that this mechanism contributes to cell survival in genotoxic stress conditions, we measured cell viability in SDOS-overexpressing and KD cells following etoposide treatment, and their response to autophagy inhibition mediated by bafilomycin, which is well-known to inhibit the process by blocking the proton pumps needed for organelle acidification[23]. Results showed that SDOS overexpression slightly increases resistance to etoposide-induced cell death, whereas SDOS silencing increases sensitivity, although in a non-statistically significant manner (Fig. 5B). Co-treatment with low doses of bafilomycin dramatically increased cell death, confirming that autophagy is used as a survival mechanism in this setting, and the most significant sensitization is shown by SDOS-overexpressing cells. Accordingly, treatment with bafilomycin alone significantly reduces viability of SDOS-overexpressing cells, whereas SDOS KD cells are the less sensitive to bafilomycin overall (Fig. 5C). Taken together, these data confirm that SDOS-expressing cells rely on autophagy as a survival mechanism, and that this confers them a survival advantage in genotoxic stress conditions.

A) Western blot of shNS and shSDOS samples treated with CHX (100 μg/mL, 4 h), etoposide (40 μM, 16 h), or both (CHX added in the last 4 hours of the 16 h-etoposide treatment). Puromycin (10 μg/mL) was added to each sample in the last 10 min before lysis. Actin was used as a normalizer. LC3B was used as an autophagy marker. The anti-puromycin hybridization shows the efficacy of CHX in blocking

translation. The graph in the right panel shows Actin-normalized densitometric quantification of SQSTM1 bands from two independent experiments. B-C) Resazurin-based viability assays in shNS and shSDOS or in H3-flag and SDOS-flag MCF7 cells after 24 hours of Tet induction followed by 48 hours of treatment with etoposide alone (40 μM) or in combination with low doses of bafilomycin (20 nM) (B), or with bafilomycin alone (C).

3.6 SDOS and SQSTM1 expression directly correlate in breast cancer but not in normal tissue

Considering the regulatory role of SDOS in DNA repair, through the interplay with 53BP1, and the relevance of DDR and autophagy regulation in BC, as well as therapeutic approaches based on drug inhibitors of both processes, we investigated the relevance of the SDOS-SQSTM1 axis in human breast tumors: to this aim a bioinformatic analysis was performed to look for the correlation between the expression levels of the two genes using GEPIA[19]. Results showed that both genes follow a path of progressive increase in expression from normal tissue, to primary tumor, to metastatic disease (Fig. 6A). Of note, SDOS and SQSTM1 mRNA expression show a significant positive correlation in the human breast cancer tissues (Fig. 6B), but no correlation at all in the corresponding normal tissues (Fig. 6C).

A) SDOS (NUDT16L1) and SQSTM1 expression in normal breast, tumor and metastatic tissues. B-C) Expression correlation between SDOS (NUDT16L1) and SQSTM1 in BC (B) and normal breast tissues (C).

4. Discussion

BC is the most common cancer globally. 2.3 million new cases and 685 thousand deaths due to BC were diagnosed in the world, only in 2020 (Sung et al., 2021). Treatment strategies for BC include chemotherapy, endocrine therapies, immunotherapy with monoclonal antibodies directed at tumor receptors, surgery, and radiation[3]. Key mechanisms of resistance to the different treatment options include alterations in DDR pathways, autophagy and other adaptive cellular responses, such as overexpression of transporters, that lead to the efflux of chemotherapeutic agents, hypoxia, or epigenetic alterations [24].

In the field of DDR, SDOS has been at the epicenter of an intensive scientific discussion due to its discovered role as a key regulator of DNA repair through its interaction with 53BP1, the master regulator of the NHEJ repair pathway. The exploration of SDOS role in the BC context opens new perspectives for understanding molecular mechanisms of tumorigenesis and resistance to treatments. Its negative regulatory role on 53BP1 has been correlated with resistance to PARPi in BRCA1- and BRCA2-mutated tumors. Furthermore, SDOS characterization as an RBP has added complexity in the characterization of its biological role. SDOS ability to interact with RNAs and modulate translation of specific transcripts suggests that there is a link between its nuclear and cytoplasmic function. In this regard, the observation that SDOS interacts with active ribosomes, coupled with the evidence that etoposide treatment reduces the amount of active polysomes in MCF7 cells independently of SDOS expression, indicates a selective translational regulatory mechanism. These data are consistent with the notion that, while overall

translation is elevated in tumors, most cancer cells reduce global mRNA translation upon stress and activate a mechanism of selective translation that contributes to tumor adaptation [25].

Previous CLIP-seq had revealed that the transcript p62/SQSTM1, a key protein in selective autophagy[20], is an mRNA target of SDOS in HeLa cells, providing a potential target of such regulation. Although we were unable to directly confirm this direct interaction, likely for the dynamic nature of this process, multiple approaches to measure selective translation allowed us to demonstrate that SQSTM1 mRNA translation is higher in SDOS KD cells compared to controls in unstressed conditions, consistent with SDOS role in repressing translation of its target mRNAs; however, upon exposure to etoposide, the translation of the SQSTM1 mRNA is sustained in SDOS-expressing cells only, against the global trend. This suggests that SDOS acts as a translational repressor under unstressed conditions, releasing protected mRNA for stress-responsive translation.

High SQSTM1 protein expression contributes to malignancy in several cancers, including epithelial ovarian cancer [26], Oral Squamous Cell Carcinoma [27], Endometrial Cancer [28], prostate cancer [29], Hepatocellular Carcinoma [30]. Intriguingly, the SQSTM1 protein overexpression in tumor tissues, but not SQSTM1 mRNA expression, was associated with a worse prognosis in several cancer types [31].

Therefore, SDOS regulation of SQSTM1 expression/activity, and especially its translation regulation, might contribute to BC chemoresistance. Our results indicate that SDOS plays a protective role in regulating SQSTM1 activity and autophagy in response to DNA damage, similar to its function in modulating 53BP1 activation in the nucleus. Therefore, the resistance to etoposide treatment of SDOS overexpressing cells may be attributed, at least in part, to increased autophagy. While autophagy is typically considered a regulator of cellular homeostasis, in established tumors it can confer a selective advantage, enhancing proliferation and promoting escape from anti-cancer therapies [32].

Several mechanisms contribute to autophagy activation, including SQSTM1 oligomerization [33]. Intriguingly, recent studies have characterized SQSTM1 as a non-canonical RBP, additionally showing that its autophagy function is regulated by the binding to the small noncoding vault RNAs[14]. Considering that the vault RNAs are also SDOS mRNA targets, according to our previous iCLIP[8], we performed RIP experiments to explore the possibility that the SDOS-SQSTM1 protein interaction could affect SQSTM1 binding to vault RNAs and represent a mechanistic model for the SDOS-mediated regulation of its activation. Results showed that upon SDOS silencing and etoposide treatment, the binding between SQSTM1 and vtRNA1-1 is indeed reduced, consistent with SQSTM1 activation. Concomitantly, SDOS is detached by SQSTM1/p62 protein, while binding vtRNA1-1 following DNA damage.

In this view, our work shows an intriguing new level of complexity, with a multiple-level regulation by a single RBP on the same target (SQSTM1): specifically, this is achieved through both regulation of translation of the mRNA and contribution to riboregulation of the mature protein. Taken together, these findings propose a model in which SDOS plays a crucial role in DNA damage response by coordinating its nuclear and cytoplasmic function. Our data integrate a model in which SDOS inhibits the translation

of specific mRNAs, including SQSTM1, and blocks 53BP1 in the nucleus under basal conditions. Conversely, DNA damage induces SDOS-53BP1 dissociation in the nucleus, allowing the activation of the NHEJ pathway, and SDOS-SQSTM1 dissociation in the cytoplasm, activating pro-survival autophagy, while promoting translation of specific mRNAs, including SQSTM1, to sustain the stress response.

In this context, the overexpression of SDOS frequently observed in tumors, and BC in particular, likely represents the crucial event for the maintenance of cellular homeostasis in the challenging tumor environment. Accordingly, SDOS and SQSTM1 are co-expressed in BC tissues and their expression increases linearly from normal tissues to tumor to metastatic disease.

Declarations

Competing Interests

The authors have no relevant financial or non-financial interests to disclose.

Acknowledgments

The authors would like to thank:the “BIOmedical iMAGIng fAcility” of the Department of Molecular Medicine and Medical Biotechnology (University Federico II, Naples, Italy); Prof. Reuven Agami (Netherlands Cancer Institute) for providing the MCF7 Flp-In T-Rex cells.

Funding

This work was supported by Fondazione AIRC per la Ricerca sul Cancro (grant MFAG-30954 to R.A.)

Data Availability

All data supporting the findings of this study are available within the paper and its Supplementary Information.

Ethics declaration: not applicable.

Author contributions

Danilo Swann Matassa and Rosario Avolio contributed to the study conception and design. Material preparation, data collection and analysis were performed by Anna Di Micco, Margherita Auriemma and Danilo Swann Matassa. The first draft of the manuscript was written by Margherita Auriemma and Danilo Swann Matassa and all authors commented on previous versions of the manuscript. All authors read and approved the final manuscript. Funding acquisition was obtained by Rosario Avolio. Supervision was provided by Danilo Swann Matassa and Franca Esposito.

References

1. H. Sung, J. Ferlay, R. L. Siegel, M. Laversanne, I. Soerjomataram, A. Jemal, and F. Bray, CA. Cancer J. Clin. **71**, 209 (2021).
2. E. Nolan, G. J. Lindeman, and J. E. Visvader, Cell **186**, 1708 (2023).
3. C. C. O'Sullivan, C. L. Loprinzi, and T. C. Haddad, Mayo Clin. Proc. **93**, 794 (2018).
4. L. M. Jackson and G.-L. Moldovan, NAR Cancer **4**, zcac042 (2022).
5. P. Drané, M.-E. Brault, G. Cui, K. Meghani, S. Chaubey, A. Detappe, N. Parnandi, Y. He, X.-F. Zheng, M. V. Botuyan, A. Kalousi, W. T. Yewdell, C. Münch, J. W. Harper, J. Chaudhuri, E. Soutoglou, G. Mer, and D. Chowdhury, Nature **543**, 211 (2017).
6. F. Maddalena, L. Sisinni, G. Lettini, V. Condelli, D. S. Matassa, A. Piscazzi, M. R. Amoroso, G. La Torre, F. Esposito, and M. Landriscina, Mol. Oncol. **7**, 895 (2013).
7. S. De Lella, L. Pedalino, M. Almagboul Abdalla Abaker, C. Mignogna, R. Cautiero, F. Esposito, D. S. Matassa, and R. Avolio, RNA rna.080588.125 (2025).
8. R. Avolio, A. I. Järvelin, S. Mohammed, I. Agliarulo, V. Condelli, P. Zoppoli, G. Calice, D. Sarnataro, E. Bechara, G. G. Tartaglia, M. Landriscina, A. Castello, F. Esposito, and D. S. Matassa, Nucleic Acids Res. **46**, 12067 (2018).
9. R. F. Ketley, F. Battistini, A. Alagia, C. Mondielli, F. Iehl, E. Balikçi, K. V. M. Huber, M. Orozco, and M. Gullerova, Cell Rep. **41**, 111526 (2022).
10. S. Kilgas, A. Syed, P. Toolan-Kerr, M. L. Swift, S. Roychoudhury, A. Sarkar, S. Wilkins, M. Quigley, A. R. Poetsch, M. V. Botuyan, G. Cui, G. Mer, J. Ule, P. Drané, and D. Chowdhury, Nat. Commun. **15**, 8438 (2024).
11. C. Theocharopoulos, P.-P. Lialios, M. Samarkos, H. Gogas, and D. C. Ziogas, Vaccines **9**, 1111 (2021).
12. J. Debnath, N. Gammoh, and K. M. Ryan, Nat. Rev. Mol. Cell Biol. **24**, 560 (2023).
13. P. Lascaux, G. Hoslett, S. Tribble, C. Trugenberger, I. Antičević, C. Otten, I. Torrecilla, S. Koukouravas, Y. Zhao, H. Yang, F. Aljarbou, A. Ruggiano, W. Song, C. Peron, G. Deangeli, E. Domingo, J. Bancroft, L. Carrique, E. Johnson, I. Vendrell, R. Fischer, A. W. T. Ng, J. Ngeow, V. D'Angiolella, N. Raimundo, T. Maughan, M. Popović, I. Milošević, and K. Ramadan, Cell **187**, 5698 (2024).
14. R. Horos, M. Büscher, R. Kleinendorst, A.-M. Alleaume, A. K. Tarafder, T. Schwarzl, D. Dziuba, C. Tischer, E. M. Zielonka, A. Adak, A. Castello, W. Huber, C. Sachse, and M. W. Hentze, Cell **176**, 1054 (2019).
15. C. A. Schneider, W. S. Rasband, and K. W. Eliceiri, Nat. Methods **9**, 671 (2012).
16. T.-S. Kim, C.-Y. Jang, H. D. Kim, J. Y. Lee, B.-Y. Ahn, and J. Kim, Mol. Biol. Cell **17**, 824 (2006).
17. E. Villanueva, T. Smith, R. M. L. Queiroz, M. Monti, M. Pizzinga, M. Elzek, V. Dezi, R. F. Harvey, M. Ramakrishna, A. E. Willis, and K. S. Lilley, Nat. Protoc. **15**, 2568 (2020).
18. C. A. H. Allard, A. B. Thies, R. Mitra, P. M. Vaelli, O. D. Leto, B. L. Walsh, E. M. J. Laetz, M. Tresguerres, A. S. Y. Lee, and N. W. Bellono, Cell **188**, 5266 (2025).
19. Z. Tang, B. Kang, C. Li, T. Chen, and Z. Zhang, Nucleic Acids Res. **47**, W556 (2019).
20. T. Lamark, S. Svenning, and T. Johansen, Essays Biochem. **61**, 609 (2017).

21. L. A. Street, M. Jovanovic, and E. F. Fornasiero, FEBS J. **293**, 3423 (2026).
22. B. Carroll, E. G. Otten, D. Manni, R. Stefanatos, F. M. Menzies, G. R. Smith, D. Jurk, N. Kenneth, S. Wilkinson, J. F. Passos, J. Attems, E. A. Veal, E. Teyssou, D. Seilhean, S. Millecamps, E.-L. Eskelinen, A. K. Bronowska, D. C. Rubinsztein, A. Sanz, and V. I. Korolchuk, Nat. Commun. **9**, 256 (2018).
23. R. Wang, J. Wang, A. Hassan, C.-H. Lee, X.-S. Xie, and X. Li, Nat. Commun. **12**, 1782 (2021).
24. N. Vasan, J. Baselga, and D. M. Hyman, Nature **575**, 299 (2019).
25. G. Leprivier, B. Rotblat, D. Khan, E. Jan, and P. H. Sorensen, Biochim. Biophys. Acta BBA - Gene Regul. Mech. **1849**, 845 (2015).
26. R. Iwadate, J. Inoue, H. Tsuda, M. Takano, K. Furuya, A. Hirasawa, D. Aoki, and J. Inazawa, Acta Histochem. Cytochem. **47**, 295 (2014).
27. Y.-K. Tseng, C.-F. Chen, C.-W. Shu, C.-H. Lee, Y.-T. Chou, Y.-J. Li, H.-H. Liou, J.-T. Cheng, C.-L. Chen, L.-P. Ger, and P.-F. Liu, Int. J. Mol. Sci. **22**, 12226 (2021).
28. R. Iwadate, J. Inoue, H. Tsuda, M. Takano, K. Furuya, A. Hirasawa, D. Aoki, and J. Inazawa, Am. J. Pathol. **185**, 2523 (2015).
29. L. Falasca, F. Torino, M. Marconi, M. Costantini, V. Pompeo, S. Sentinelli, L. De Salvo, M. Patrizio, C. Padula, M. Gallucci, M. Piacentini, and W. Malorni, Apoptosis **20**, 1577 (2015).
30. A. Abdel-Moety, N. Baddour, P. Salem, H. El-Tobgy, and A. El-Shendidi, J. Clin. Exp. Hepatol. **12**, 774 (2022).
31. L. Zhu, Y. Wang, J. He, J. Tang, W. Lv, and J. Hu, J. Cancer **9**, 4072 (2018).
32. S. Patergnani, S. Missiroli, G. Morciano, M. Perrone, C. M. Mantovani, G. Anania, F. Fiorica, P. Pinton, and C. Giorgi, Cancers **13**, 5622 (2021).
33. R. Ciuffa, T. Lamark, A. K. Tarafder, A. Guesdon, S. Rybina, W. J. H. Hagen, T. Johansen, and C. Sachse, Cell Rep. **11**, 748 (2015).

Figures

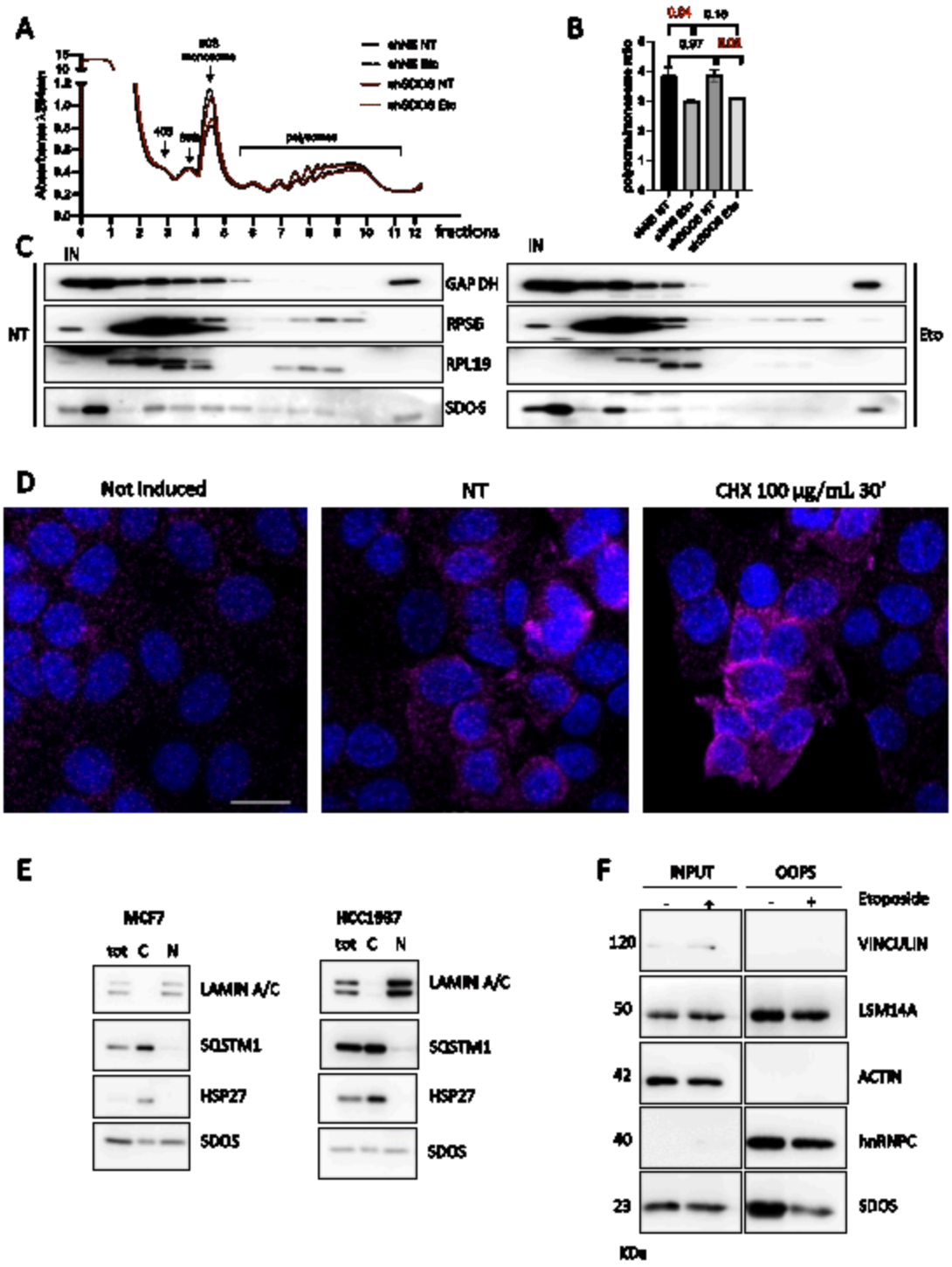


Figure 1

SDOS is associated with actively translating polysomes and binds RNAs in BC cells

(A) Polysome profiling, with absorbance measurement at 254 nm, of MCF7 clones silenced for SDOS (shSDOS) and its control shNS, in the presence and absence of 4-hour treatment with 40 µM etoposide (Eto). The peaks in the profile, from left to right, reflect ribosomal protein complexes with increasing density: free ribonucleoproteins, small (40S) and large (60S) ribosomal subunits, monosomes (80S), and polysomes. The area under the curve corresponding to fractions 5 and 6 represents the monosomes,

while the area from fractions 7 to 12 indicates the polysomes. (B) The graph shows the polysome/monosome ratio as a measure of translational activity. The numbers on the bars indicate statistical significance, calculated using Student's t-test (n = 3). (C) Western blot analysis of fractions extracted from the polysome profiling of untreated MCF7 shNS cells (NT) and cells treated for 4 hours with etoposide 40 μM (Eto), along with their respective inputs (IN). Probing was performed with anti-GAPDH, representing a cytosolic protein that should not be associated with polysomes, anti-RPS6, as a marker of the ribosomal small subunit, anti-RPL19 as a marker of the ribosomal large subunit, and anti-SDOS antibodies. (D) Representative image of PLA showing the interaction of SDOS-flag with phosphorylated (active) ribosomal protein S6 (phosphoRPS6) in MCF7 cells following 24 h induction of SDOS-flag by using anti-FLAG and anti-phosphoRPS6 antibodies. Positive signals of interaction are shown as pink dots, nuclei are stained with DAPI (blue). Cycloheximide (CHX) treatment (100 μg/mL, 30 min) was used to stabilize the binding ribosome and increase binding. Scale bar: 20μm. E) Subcellular fractionation performed in MCF7 (left) and HCC1937 (right) BC cells, to identify total (tot), cytosolic (C) and nuclear (N) pools of the SDOS protein. Lamin A/C have been used as nuclear markers, HSP27 has been used as a cytosolic marker. F) Representative western blot of OOPS samples after 4-hour treatment with etoposide (40 μM) and respective inputs. Vinculin and Actin were used as negative controls (being proteins that do not bind RNAs), while the two canonical RBPs LSM14A and hnRNPC were used as positive controls, to confirm quality of RBP isolation.

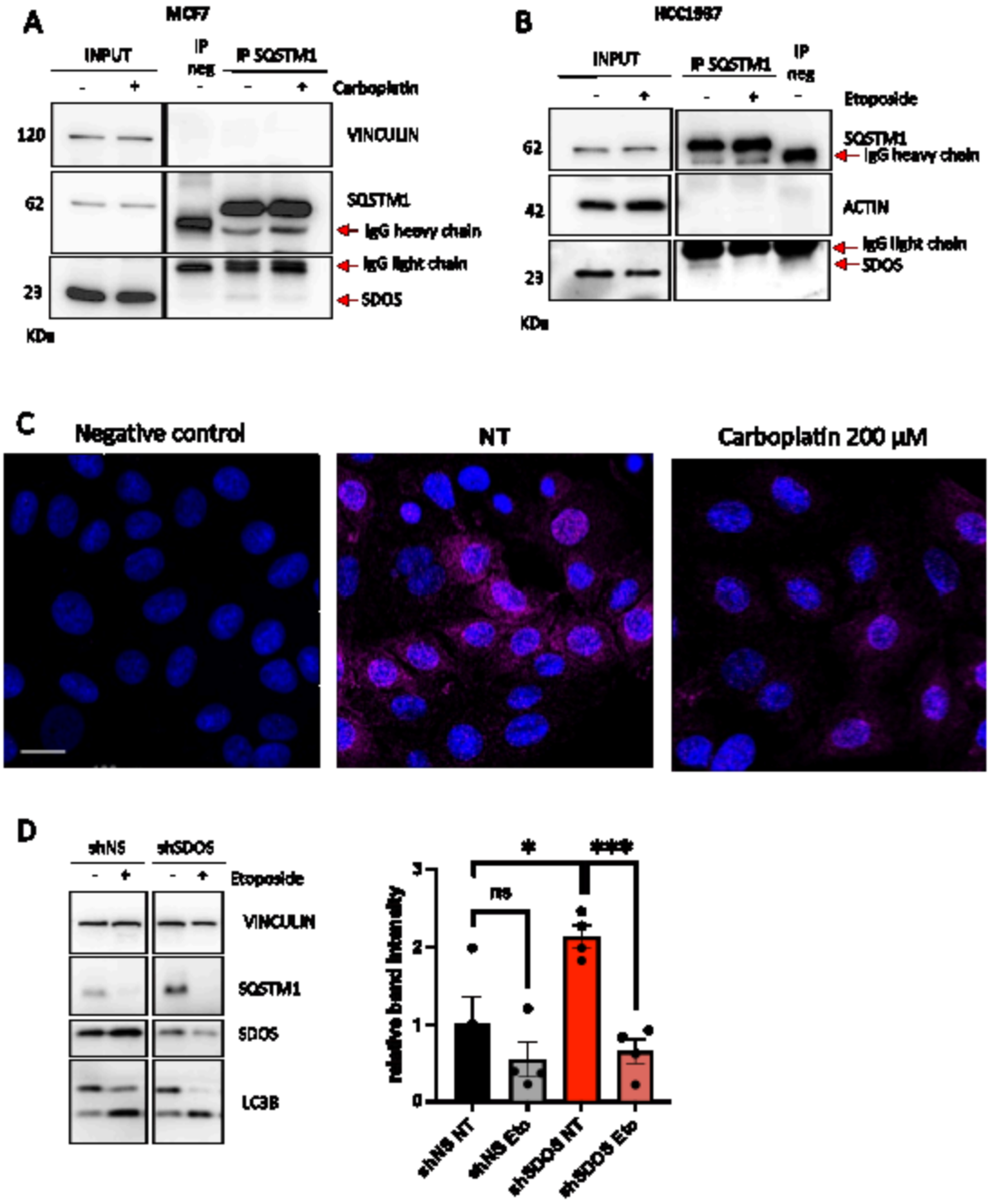


Figure 2

SDOS binds SQSTM1/p62

A) MCF7 cells were treated for 4 hours with Carboplatin (400 µM), harvested and total lysates were immunoprecipitated with anti-SQSTM1 antibodies. VINCULIN was used as a loading control. B) HCC1937 cells were treated with etoposide (20 µM) for 1 hour, harvested, and total lysates were immunoprecipitated with anti-SQSTM1 antibodies. ACTIN was used as a loading control. C) Representative image of PLA showing the interaction of SDOS-flag with SQSTM1/p62 in MCF7 cells following 24 h induction of SDOS-flag using anti-FLAG and anti-SQSTM1 antibodies. Positive signals of interaction are shown as pink dots, nuclei are stained with DAPI (blue). Scale bar: 20µm. D)

Representative Western blot of shNS and shSDOS samples treated with etoposide (40 μM) for 16 hours, compared to their respective untreated controls. Vinculin was used as a normalizer. LC3B was used as an autophagy marker. The bar graph shows mean ± SEM of densitometric quantification of normalized SQSTM1 bands in three replicates. Asterisks represent the statistical significance based on a Student's t-test. *= p<0.05; ***= p<0.001.

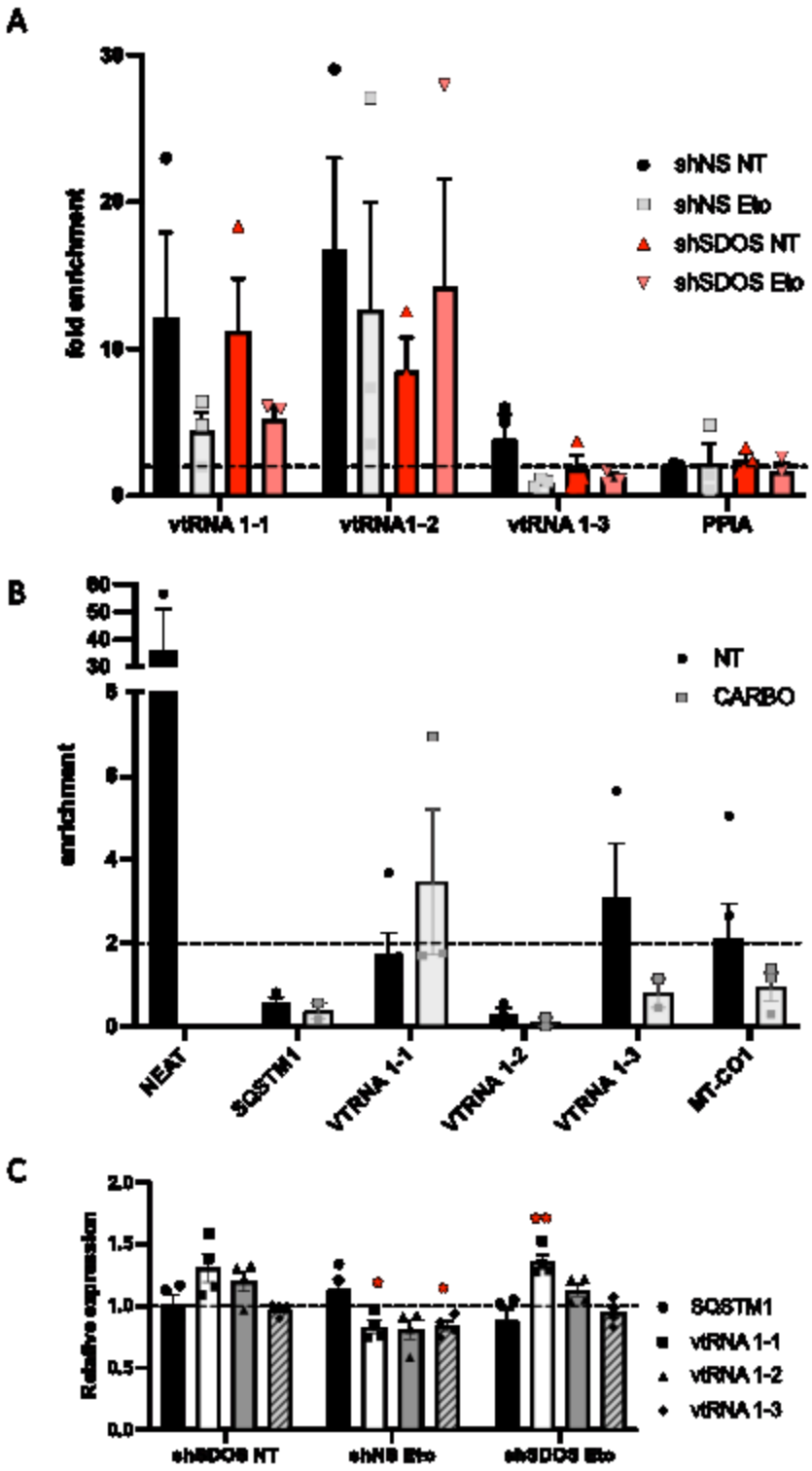


Figure 3

SDOS regulates SQSTM1 activation through its binding to vtRNAs

A) RIP-qPCR assays performed in shNS and shSDOS cells treated for 1 hour with 40 µM etoposide. The data are represented as mean ± SEM of three independent experiments. B) RIP-qPCR assays performed in SDOS-flag MCF7 cells treated for 4 hours with 400 µM Carboplatin. The data are represented as mean ± SEM of five independent experiments. C) RT-qPCR of total RNAs extracted from shNS/shSDOS MCF7 cells, after 72 hours of induction followed (where indicated) by a 4-hour etoposide treatment (40 µM). Data represent mean ± SEM of four independent experiments. Asterisks show statistical significance (*p<0.05; **p<0.01) based on the Student's t test.

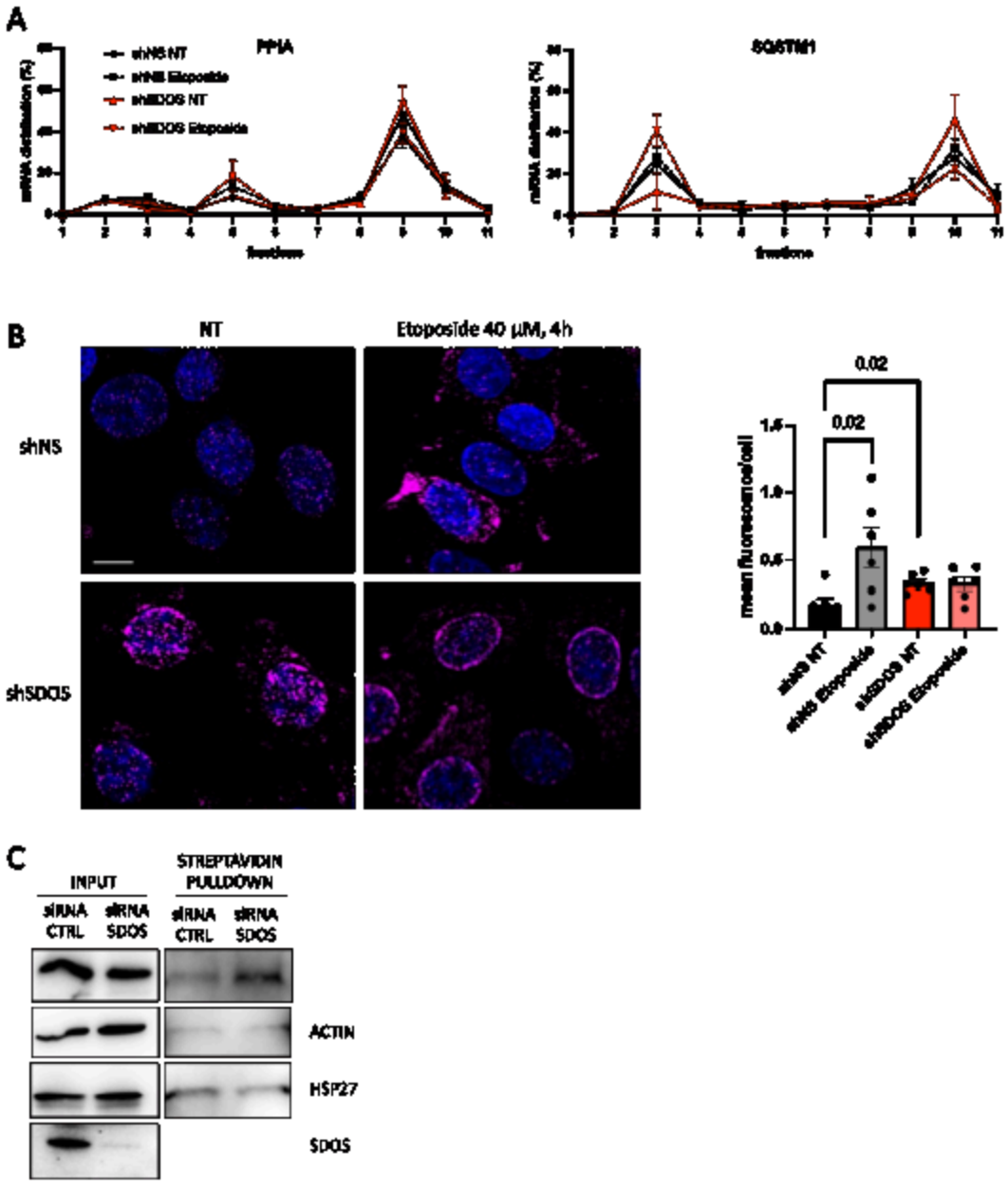


Figure 4

SDOS regulates SQSTM1 mRNA translation

A) Distribution of the mRNAs in a polysome profile. Data are represented as mean ± SEM of three independent experiments and have been obtained by amplifying by RT-qPCR the indicated transcripts from every single fraction collected in a polysome profiling experiment and calculating the percent distribution of the transcript along the gradient. 100 pg of Luciferase mRNA have been added as a spike-in control to each fraction and later used as a reference in the RT-qPCR assay. Fractions 7-11 represent the active polysomal fractions. B) Representative image (left) and fluorescence intensity quantification (right) of puro-PLA performed by adding low doses of puromycin (1 µg/mL) for 10 minutes to shNS and shSDOS MCF7 cells following treatment with etoposide (40 µM, 4h) and controls before fixation. Pink dots represent the puromycylated nascent chains of the SQSTM1 protein. Nuclei are stained with DAPI (blue). Scale bar: 10µm. The bar graph shows fluorescence intensity quantification represented as mean ± SEM of 6 fields from two biologically independent replicates. Numbers above bars show statistical significance (p-values) on an unpaired t-test.

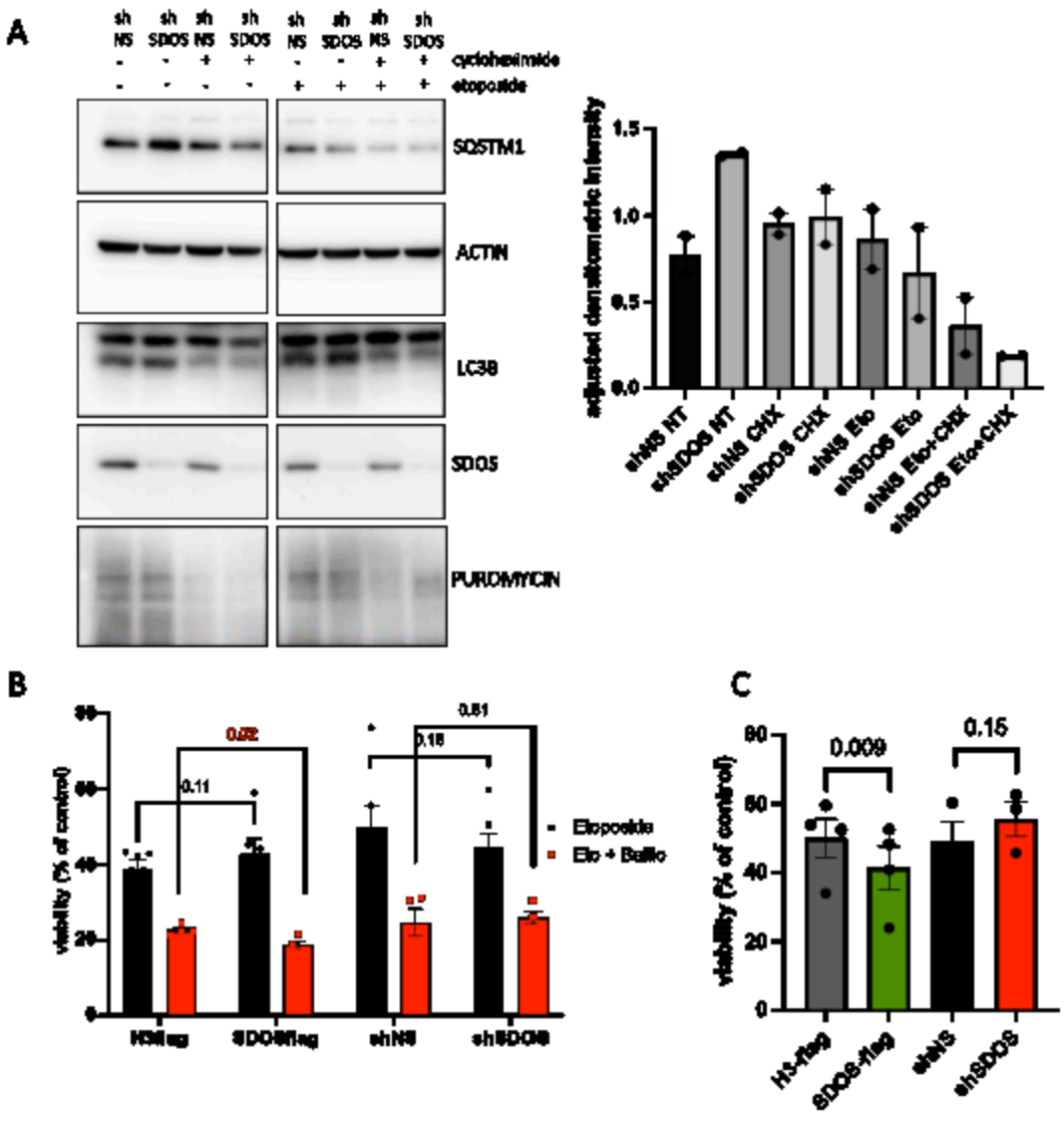


Figure 5

SDOS regulates SQSTM1 expression and activity

A) Western blot of shNS and shSDOS samples treated with CHX (100 µg/mL, 4 h), etoposide (40 µM, 16 h), or both (CHX added in the last 4 hours of the 16 h-etoposide treatment). Puromycin (10 µg/mL) was added to each sample in the last 10 min before lysis. Actin was used as a normalizer. LC3B was used as an autophagy marker. The anti-puromycin hybridization shows the efficacy of CHX in blocking translation. The graph in the right panel shows Actin-normalized densitometric quantification of SQSTM1 bands from two independent experiments. B-C) Resazurin-based viability assays in shNS and shSDOS or in H3-flag and SDOS-flag MCF7 cells after 24 hours of Tet induction followed by 48 hours of treatment with etoposide alone (40 µM) or in combination with low doses of bafilomycin (20 nM) (B), or with bafilomycin alone (C).

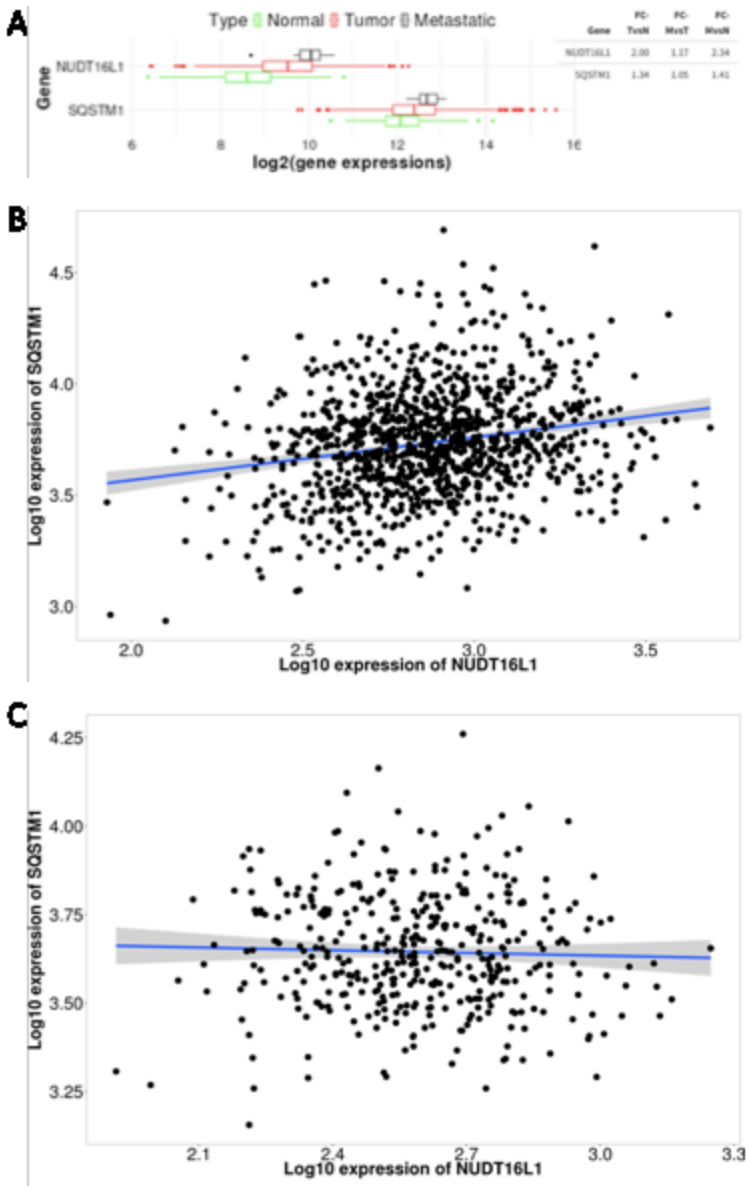


Figure 6

SDOS and SQSTM1 are co-expressed in human breast tumors

A) SDOS (NUDT16L1) and SQSTM1 expression in normal breast, tumor and metastatic tissues. B-C) Expression correlation between SDOS (NUDT16L1) and SQSTM1 in BC (B) and normal breast tissues (C).

Supplementary Files

This is a list of supplementary files associated with this preprint. Click to download.

- SupplementaryFigS1.pdf
- uncutblotsDiMiccoetal.pdf